Available online at www.sciencedirect.com
SCIENCE DIRECT®
Nuclear Instruments and Methods in Physics Research A 498 (2003) 155–164
NUCLEAR INSTRUMENTS & METHODS IN PHYSICS RESEARCH Section A
www.elsevier.com/locate/nima

Neutron recoils in the DRIFT detector

D.P. Snowden-Ifft[a,b,*], T. Ohnuki[a,b], E.S. Rykoff[a,b], C.J. Martoff[a,b]

[a] Physics Department, Occidental College, 1600 Campus Road, Los Angeles, CA 90041, USA
[b] Barton Hall, Temple University, 1900 N. 13th St., Philadelphia, PA 19122-6082, USA

Received 5 July 2002; received in revised form 11 October 2002; accepted 27 November 2002

Abstract

The Directional Recoil Identification From Tracks (DRIFT) project is an endeavor to build and operate a low pressure negative ion TPC to search for weakly interacting massive particles thought to make up the dark matter in our Galaxy. This paper will focus on a neutron exposure of a small DRIFT prototype, a Monte Carlo to simulate these events, and the derivation of the range and ionization as a function of energy for Sulfur and Carbon recoils in CS_2 gas.

PACS: 29.40.Cs; 29.40.Gx; 28.20.Cz; 95.35.+d

Keywords: Range; Ionization; Dark matter; Negative ion

1. Introduction

The Directional Recoil Identification From Tracks (DRIFT) detector is a low pressure Negative Ion TPC (NITPC) designed to detect Weakly Interacting Massive Particles (WIMPs) a prime dark matter candidate. A description of the capabilities of a low pressure NITPC for WIMP detection can be found in Ref. [1]. The NITPC technique relies on the drifting of negative ions, instead of electrons, to reduce diffusion in all dimensions eliminating the need for a large magnet. This idea has been thoroughly validated in Refs. [2,3]. A DRIFT prototype was exposed to neutrons from a ^{252}Cf source to calibrate the response of the detector to recoiling ions. The data from that experiment, including anisotropy measurements, and a Monte Carlo (MC) which well simulates the data will be presented here. Specifically the data and MC were used to derive the range and ionization as a function of energy for C and S recoils in CS_2 gas.

2. Experimental procedure and data

The exposure was carried out at the Kellogg Radiation Facility at Caltech. The source of the neutrons was a ~3.75-year-old ~2 mCi ^{252}Cf source encapsulated in a double walled stainless steel container approximately 5 cm high × 1.5 cm wide [4]. This source slid up and down an aluminum tube slightly larger than its width. The tube was surrounded by paraffin. A hole in the

*Corresponding author. Physics Department, Occidental College, 1600 Campus Road, Los Angeles, CA 90041, USA. Tel.: +1-323-259-2793; fax: +1-323-259-2704.
E-mail address: ifft@oxy.edu (D.P. Snowden-Ifft).

0168-9002/03/$ - see front matter
doi:10.1016/S0168-9002(02)02120-4

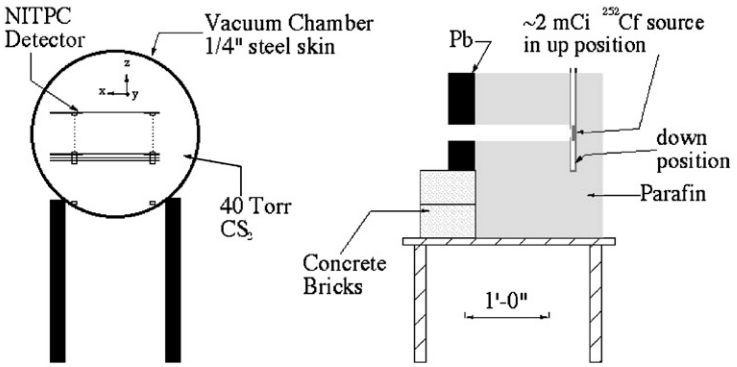

Fig. 1. Experimental setup for the neutron exposure.

aluminum tube and paraffin allowed neutrons to pass to the detector when the neutron source was in the up position, see Fig. 1.

The NITPC detector, see Fig. 2, used in this experiment sat in the middle of a 2′ diameter 3′ long cylindrical vacuum vessel as shown in Fig. 1. In a typical run the vacuum vessel would be evacuated to ~ 100 mTorr and then backfilled to a pressure of 40 Torr with CS_2 and sealed for the duration of the run. The detector consisted of a drift region attached to a multi-wire proportional chamber (MWPC). The drift region was composed of a cathode made from 100 μm 304 stainless steel wire on a 2 mm pitch and a field cage made of 11 loops of 100 μm 304 stainless steel wire spaced by 1/2″ These loops were supported by 8 acrylic posts on the corners of a $\sim 11'' \times \sim 11''$ square and electrically connected by a ladder of 20 MΩ (1%) resistors. The drift distance, from the cathode to the grid plane, was 6″. The MWPC was made of three wire planes, two grid planes sandwiching an anode plane. The grid and anode wires were 100 and 20 μm 304 stainless, respectively, both on a pitch of 2 mm. Anode and grid wires were oriented perpendicular to each other with a gap of 1.1 cm. All wires were mechanically and electrically attached to PCBs which had $9'' \times 9''$ holes in them filled from side to side with wires. Using an ^{55}Fe source prior to the experiment the active region of the MWPC was found to be $7'' \times 7''$. Within this region the variations of the gain were less than 5% and the fall off from full gain to $\frac{1}{2}$ gain at the edges was $\ll 1''$. A Bertan 380X in series with a RC filter

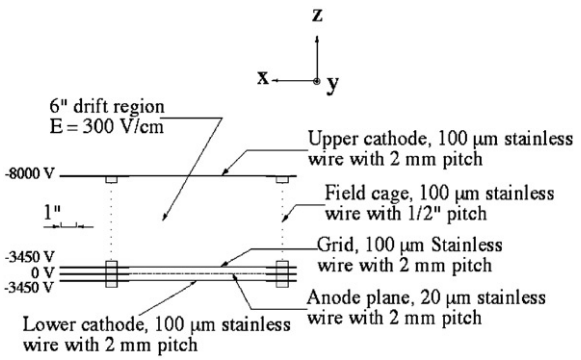

Fig. 2. Diagram of the NITPC detector used in the experiment.

to remove ripple supplied −8000 V DC to the cathode and top of the field cage resistor ladder. A 100 MΩ (1%) resistor in series with this ladder supplied −3450 V to the grids giving a drift field of 300 V/cm. The drift velocity of negative CS_2 anions in this field was found to be 2800 cm/S [3]. The anode was at ground potential.

The anode wires were summed 8 to 1 on the PCBs. These lines were connected to Amptek A250 pre-amplifiers then to Ortec 885 amplifiers with a shaping time constant of 3 μS, see Fig. 3. Because this detector utilized slowly drifting anions the events were spread out in time of order ~ 100 μS. To form a trigger based on the total ionization of the event the lines were summed using a modified Ortec 533 and then passed through an RC circuit with a time constant of 200 μS. A TTL pulse was then formed off of the

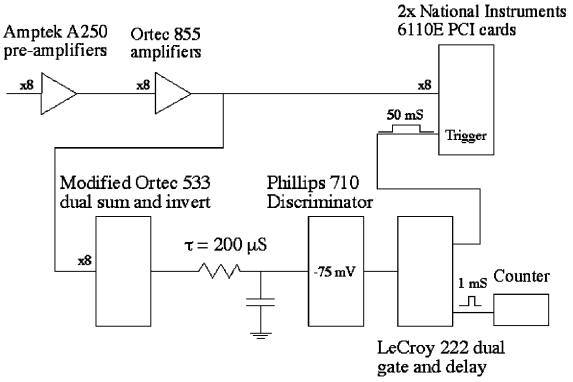

Fig. 3. Schematic of the electronics used in the neutron exposure.

Table 1
Description and characteristics of the various types of run

Type of cycle	Shadow bar	^{252}Cf	^{55}Fe	Ortec 855 Gain	Typical rates (Hz)
Calibration	In	Down	Up	200	350
Gamma	In	Up	Down	50	50
Neutron	Out	Up	Down	50	60

discriminated signal (−75 mV threshold) using a dual gate and delay generator and used to trigger two National Instruments 6110E PCI cards simultaneously. A separate, shorter TTL pulse went to a counter. The 6110E cards digitized all 8 incoming signals at 2.5 MHz for 1 mS with 4.9 mV resolution.

Runs were done in two orientations. In the "optimal" orientation (optimal because recoils traversed the most anode wires in this orientation) the neutrons traveled mostly parallel to the anode plane and perpendicular to the anode wires. In the "anti-optimal" orientation the detector was rotated 90° around an axis perpendicular to the wire planes and the neutrons traveled mostly parallel to the anode plane and parallel to the anode wires. For each orientation three different cycles were repeated. Table 1 shows the characteristics of each cycle. The shadow bar was a piece of paraffin which fit into the hole in the paraffin shown in Fig. 1 to block neutrons. Calibrations were carried out using a 100 μCi ^{55}Fe source mounted on the end of a long throw solenoid ~30 cm away from the center of the detector. In the up position this source was shielded with several layers of aluminum foil (to lower the interaction rate) and in the down position it was shielded behind ~3 mm of stainless steel. The rates for all runs were measured on the counter shown in Fig. 3.

3. Data analysis

Fig. 4 shows some typical events. For each of the eight lines a number of statistics were generated. One input required to do this analysis is a software threshold. This appears as a horizontal line on the graphs of Fig. 4. A partial list of statistics generated for each line with voltages below this software threshold follows:

V_{min} and V_{max}—the maximum and minimum voltages on a line.
Crossings—the number of times the voltage crossed the software threshold.
t_{min} and t_{max}—t_{min} is the time of the first zero crossing before the first crossing of the software threshold and t_{max} is the time of the first zero crossing after the last software threshold crossing. These times are marked with a vertical hash mark on the lines in Fig. 4.
Σ—the integral of the voltage with respect to time between t_{min} and t_{max} multiplied by −1.
NFFWHM—Negative First Full-Width at Half-Maximum. Starting at V_{min} the first occurrence of a full-width at half-minimum.
P_{lower}, P_{center}, and P_{upper}—for each line for which *Crossings* > 6 a fast Fourier analysis was done on that line and the power at three frequencies $\nu_{lower} = 6.1$ kHz, $\nu_{center} = 13.4$ kHz, and $\nu_{upper} = 18.3$ kHz were saved.

From these statistics a number of cuts were then made on the data. First, any line for which $V_{max}/|V_{min}| > 1$ was eliminated from further analysis. This *ReboundCut* eliminated lines with only induced pulses on them such as lines 3 and 6 in Fig. 4(a). For lines cut with the *ReboundCut* the Σ variable was set to zero for further analysis. After this the following cuts were placed on the data. The percentages in the parentheses will be discussed shortly.

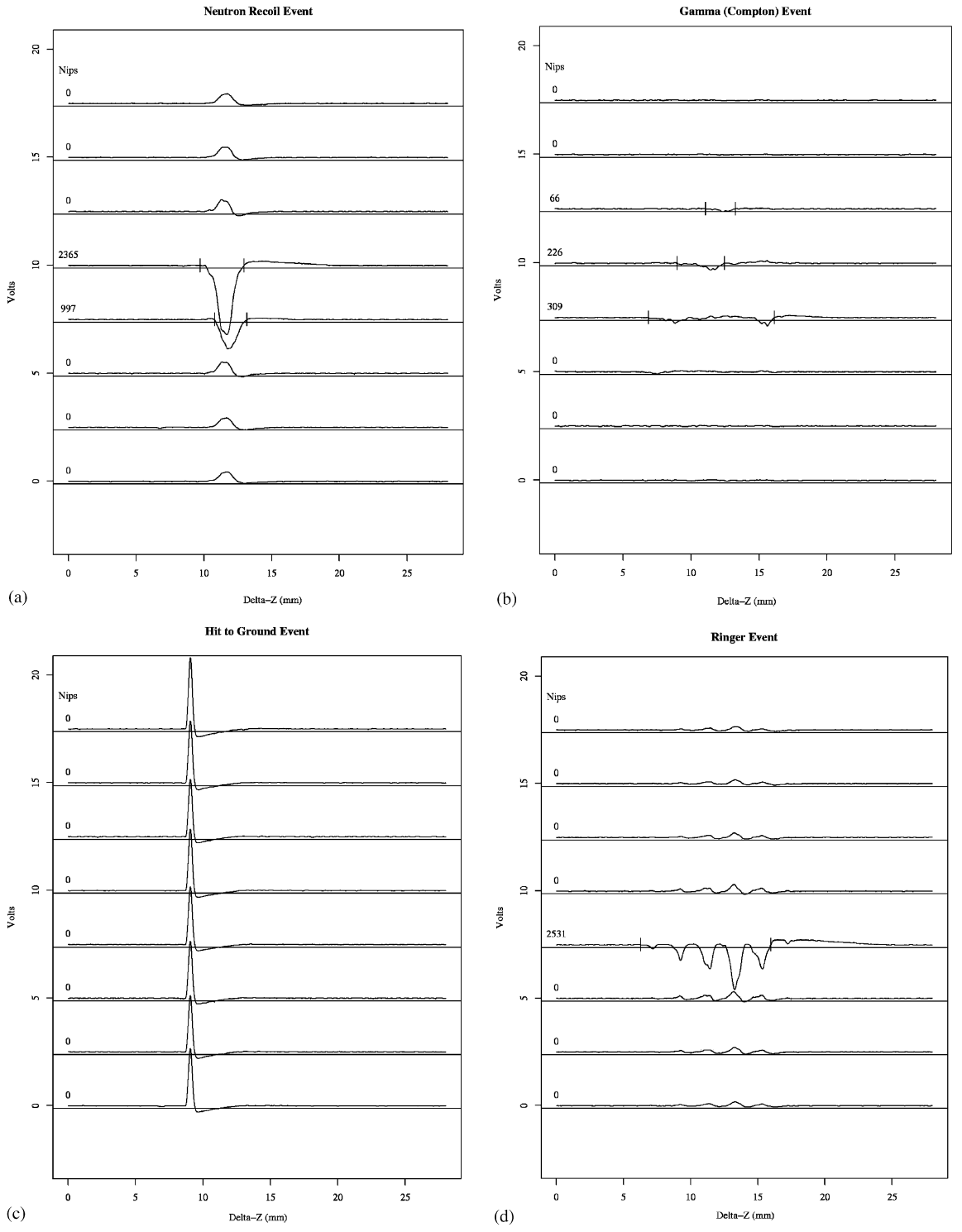

Fig. 4. Some examples of events. A constant voltage was added to each line to allow them to be printed on the same graph. Negative voltages from these baselines indicate charge depositing on the anode wires. Lines are arranged sequentially from bottom to top. The horizontal axis is time (1 mS full scale) multiplied by the drift speed.

HitToGroundCut (71%/0.043%/0.15%). Eliminated any event in which the maximum voltage exceeded +3 V on any line. Events like this occurred when a spark from the detector hit ground. An event which was eliminated by this cut is shown in Fig. 4(c).

ZeroNipCut (21.5%/52.5%/25.8%). Eliminated any event in which the sum of the Σ's for all lines was zero. This could occur despite the hardware trigger conditions because of the *ReboundCut* or because of a high software threshold.

SparkCut (6.2%/5.9%/4.0%). Cut any event in which any line had a NFFWHM $<20\,\mu$S (0.56 mm in Fig. 4). For comparison the 3 μS shaping time of the Ortec 855 amplifiers causes an instantaneous deposition of ionization to have a 9 μS NFFWHM.

SparkNearbyCut (1.4%/1.8%/2.1%). Eliminated any event which had two minima within 2 μS (0.056 mm in Fig. 4) of each other. Both this and the *SparkCut* were found useful in eliminating events which were presumed to be due to small sparks traveling between the grid and anode planes. In addition these cuts eliminated any ionization radiation which entered the drift region through the MWPC because the charge collection inside the MWPC was so rapid.

EightWireCut (0.92%/0.0%/11.3%). Eliminated any event in which eight wires received Σ's > 0.

AdjacentCut (0.74%/0.0%/0.0%). Required that lines with non-zero Σ's be adjacent to each other.

ClippingCut (0.55%/5.2%/2.2%). Eliminated any event in which $V_{\max} > 6.5$ V or $V_{\min} < -6.4$ V for any line as this indicated clipping by the amplifiers.

TimeMinCut and *TimeMaxCut* (0.55%/0.0%/11%). Required that the lines which passed the *ReboundCut* all have $t_{\min} > 0$ and $t_{\max} < 1$ mS. This cut crudely eliminated events which were not contained in the 1 mS sampling time of the data acquisition system.

RingerCut (0.02%/0.0%/1.5%). Eliminated any event in which $P_{\text{center}}/((P_{\text{lower}} + P_{\text{upper}})/2.0) > 3.0$. The event shown Fig. 4(d) was typical of a class of events called "ringers" which produce a peak in the Fourier analysis of a line which can be identified with this cut. The origin of these events is still under investigation. They are presumed not to be due to neutron recoils and were removed with the *RingerCut*.

Other cuts accounted for the remaining (2.21%, 0.0%, 22.3%).

4. *Nips* and R_2

Exposure of the detector to ^{55}Fe 5.9 keV X-rays during the calibration cycles allowed the gas gain to be calibrated. These runs were analyzed with the *ClippingCut*, *HitToGroundCut* and *RingerCut* implemented which produced a peak in the sum of the Σ variables (Σ_{total}) with a resolution of ~25%. Over the course of the experiment this peak varied by ~25%. It is known [5] that this peak corresponds to 300 ± 40 electron–ion pairs. The number of ion pairs produced by an event will hereafter be known as *Nips*. Work [5] with single electrons in CS_2 allows a calibration of the gas gain. The gas gain during this experiment was ~650. Other work [5] has shown that Σ_{total} is proportional to the *Nips* associated with an event. Thus using the average Σ_{total} for the events in the ^{55}Fe peak the Σ values for runs immediately following the calibration run were converted into *Nips*. These data are shown along the left in the graphs in Fig. 4. Summing these numbers for each event gave the total ionization (*Nips*) for the event.

Information was also available about the range of the event. Because no start pulse was associated with the events and because the lines were summed no information was available about the absolute position (x, y, and z) of the beginning of an event. In addition, because of the setup and electronics no information was available about Δy, the extent of the event along the wires (see Fig. 2 for coordinate system). Information was, however, available for Δx and Δz. Δx was taken to be the number of wires with non-zero *Nips* minus one times the wire pitch, 2 mm. For most events this underestimates the extent of the track in the x direction. Δz was taken to be the difference between the largest $t_{\max}$ of all the lines with non-zero *Nips* and the smallest $t_{\min}$ of all the lines with non-zero *Nips* times the drift velocity. Because of diffusion of the ions this procedure overestimates

Δz. From these two parameters a new parameter was formed, $R_2 = \sqrt{\Delta x^2 + \Delta z^2}$.

5. Optimizing the software threshold for neutron detection

In order to give physical meaning to the software threshold voltage the gas gain and electronic amplification were used to calculate the instantaneous deposition of *Nips* (*DFNips* for delta function *Nips*) to a wire necessary to achieve the software threshold voltage. Fig. 5(a) shows the plot of *Nips* vs. R_2 for all of the optimal neutron runs analyzed with a software threshold of 25 *DFNips* and all of the cuts discussed above implemented. As can be seen in this figure there is a band of events which is nearly vertical and one which is nearly horizontal. Fig. 5(b) shows data taken with the shadow bar in place. This paraffin shielding has the effect of absorbing the neutrons with less effect on the numerous gammas coming from the ^{252}Cf source. As can be seen in this figure the nearly horizontal band of events has disappeared. For this reason it is natural to assume that the vertical band of events is due to gammas while the horizontal band is due to neutrons. The event shown in Fig. 4(a) was selected from the neutron band while the event shown Fig. 4(b) was selected from the gamma band.

As discussed in Ref. [1] gamma events (10–20 keV electrons) travel much further than nuclear recoils for a fixed amount of ionization. Gamma events, due to the fact that the ionization is so spread out, typically have small $|V_{\min}|$, Fig. 4(b). This suggests an important mechanism for reducing gamma events from the data sample. To this end the software threshold was raised from 25 *DFNips* to 150 *DFNips*. In doing so the number of gamma events (defined as having *Nips* < 500 and $R_2 > 0.5$ cm) decreased from 413 to 0 while the number of neutron events (defined as having *Nips* > 500) decreased by only 10%. The

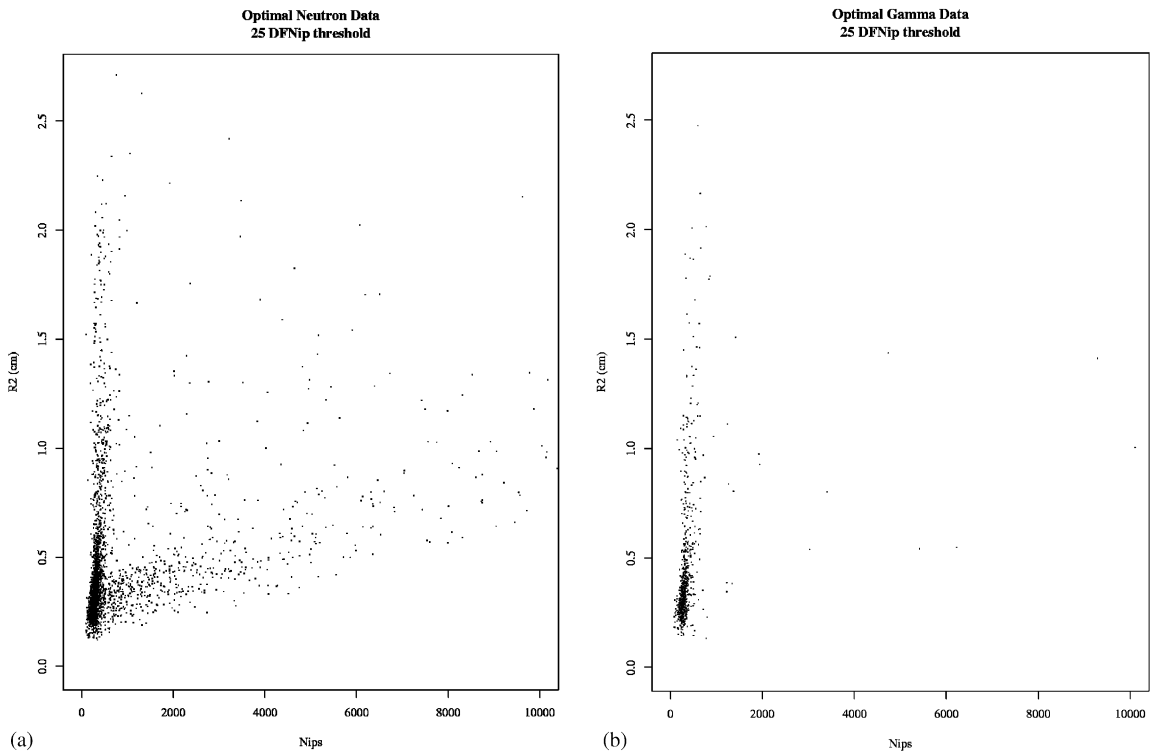

Fig. 5. Combined data (*Nips* vs. R_2) from all of the optimal neutron runs (a) and optimal gamma runs (b) with a 25 *DFNip* threshold.

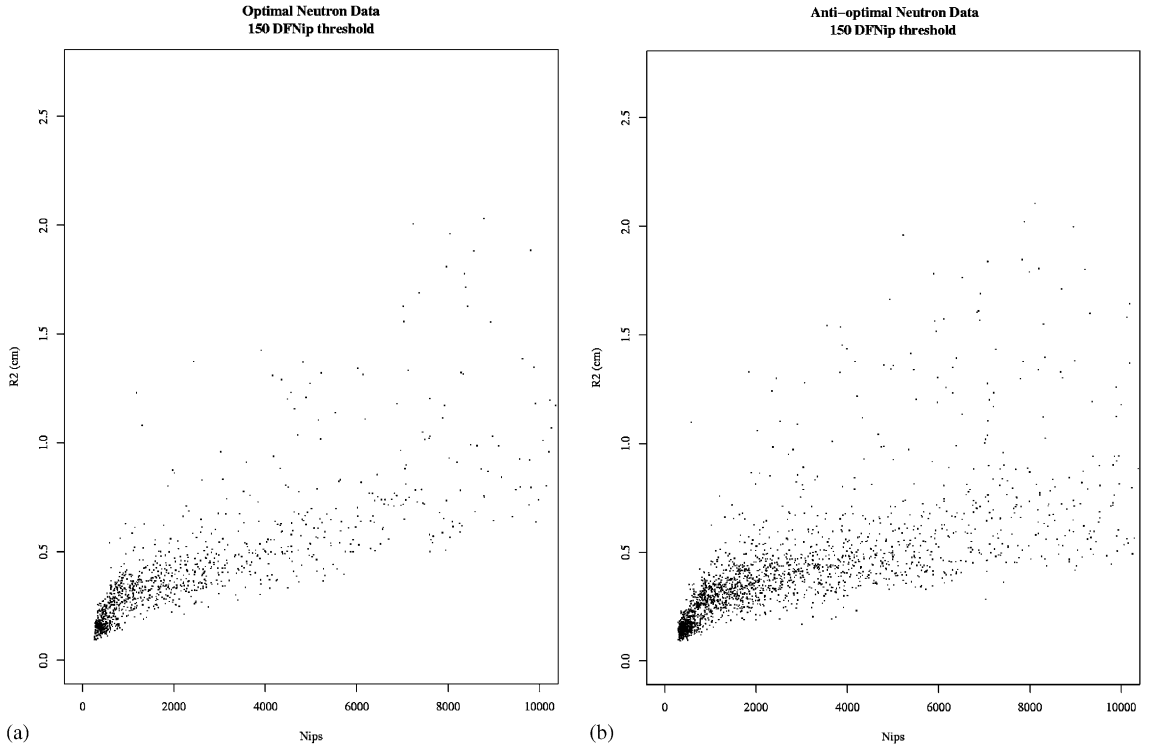

Fig. 6. Combined data (*Nips* vs. R_2) from all of the optimal neutron runs (a) and anti-optimal neutron runs (b) analyzed with a 150 *DFNip* threshold.

inherent ability of a low pressure NITPC detector to distinguish low energy electrons from low energy nuclear recoils is an important asset.

Following the name of the cuts above are the percentages of events eliminated by that cut with a 150 *DFNip* threshold. The first of these was calculated from a neutron cycle in the optimal orientation. Note that the percentages are not independent. Many events were removed by multiple cuts. Only 2% of the events in this cycle survived all of the cuts. As shown above the majority of events in this cycle were caused by hits to ground. This was presumably due to the proximity of the detector (the top of which is at −8000 V) to the grounded vacuum vessel, see Fig. 1. Fig. 6(a) shows the *Nips* vs. R_2 plots for the combined data from the optimal runs while Fig. 6(b) shows the anti-optimal data for a 150 *DFNip* threshold.

6. Asymmetry measurements

As alluded to above optimally oriented neutrons are expected to produce recoils which traverse more wires than anti-optimally oriented neutrons. This hypothesis was confirmed in the following way. Data within windows 500 *Nips* wide were selected from the optimal and anti-optimal data sets shown in Fig. 6. The mean Δx was then calculated for events in these windows. The results are shown in Fig. 7. Every single optimal data point (filled circles) lies above the corresponding anti-optimal data point (open circles), in some cases by many standard deviations, confirming the hypothesis that optimally oriented neutrons, on average, produce recoils with higher Δx than do anti-optimally oriented neutrons. Thus a low pressure NITPC can be used as a directional neutron detector.

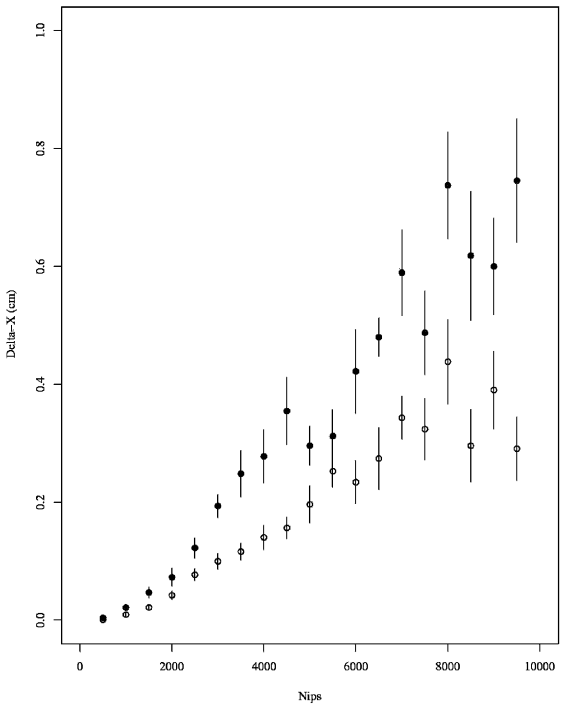

Fig. 7. Mean Δx as a function of *Nips*. The black circles show data taken from the optimal neutron runs while the open circles are from data taken from the anti-optimal neutron runs.

7. The model

A Monte Carlo (MC) has been written to simulate the neutron recoils in this experiment. The shape of the input neutron spectrum was taken to be

$$N(E) \propto \sqrt{E} e^{-E/T}$$

with $T = 1.3$ MeV from Ref. [6]. Neutrons in the MC were assumed to travel horizontally through the drift region of the detector with constant flux and a small angular spread determined by the geometry of the experiment. Differential elastic scattering cross-sections for neutrons on S and C were taken from Ref. [7]. Ranges from Ref. [8] for ions in Ar were scaled to 80 Torr to estimate ranges of S and C in 40 Torr CS_2 (80 Torr Ar has roughly the same electron density as 40 Torr CS_2). Straggling in the form of longitudinal and lateral Gaussian root mean squares of the ions were taken from SRIM97 [9] and scaled to the proper range. Straggling of the ions was added onto the nominal ranges and straight lines approximated the trajectory of the ions. The *Nips* were estimate using data found in Ref. [10] for ions in Ar and scaled by 26 eV/19 eV, the measured W factors for Ar and CS_2 [5]. *Nips* were uniformly distributed along the straight tracks. The capture distance for the electrons was assumed to be zero and diffusion was thermal in x, y, and z as indicated by Ohnuki [3]. Avalanches by single ions falling on the wires were generated using

$$P(n) = \frac{1}{G} e^{-n/G},$$

where $P(n)$ is the probability of n electrons falling on an anode wire and is only a function of the gas gain, G, of the detector. This has been found to well approximate the distribution for chambers with small gains [11]. The time profile of the voltage on a line from a single avalanched *Nip* was assumed to be Gaussian with a maximum indicated by the above equation and the electronic gain of the data acquisition system and a rms of 4.67 μS due to the Ortec 855 amplifiers. The voltages generated in this way for single *Nips* were added together for all times. Noise at an appropriate level and smoothed using the rms of the amplifiers was added to each wire. Induced pulses were generated using a fraction, −0.12, for adjacent wires and another fraction, −0.08, for the other wires. The noise and induced pulse parameters were measured from a sample of events. An example of a sulfur and carbon recoil generated in this way is shown in Fig. 8.

The advantage of this MC, over that of Snowden-Ifft [1], is that the events are generated in such a way as to mimic the data from the National Instruments boards. These "events" can then be run through the same analysis code as the raw data. Any biases to the data introduced by this analysis will then be transmitted in the same way to the MC "data". Two comparisons of the data from optimal orientation of the experiment and the "data" from the MC were then made. The first was to compare a histogram of the *Nips* from the data for events with > 500 *Nips* and with windows of 500 *Nips* to a similar histogram made from the MC "data." The reduced χ^2 for this comparison was 0.69. Next the average Δx within these *Nip*

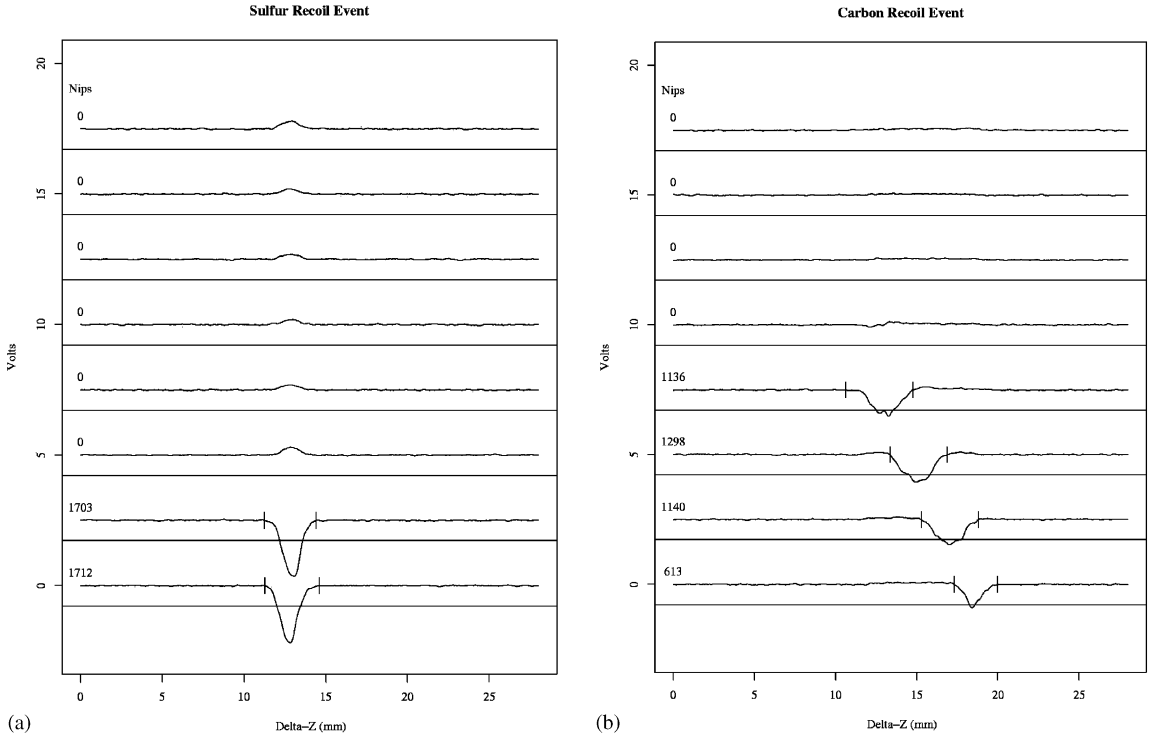

Fig. 8. Monte Carlo generated S (a) and C (b) recoil events.

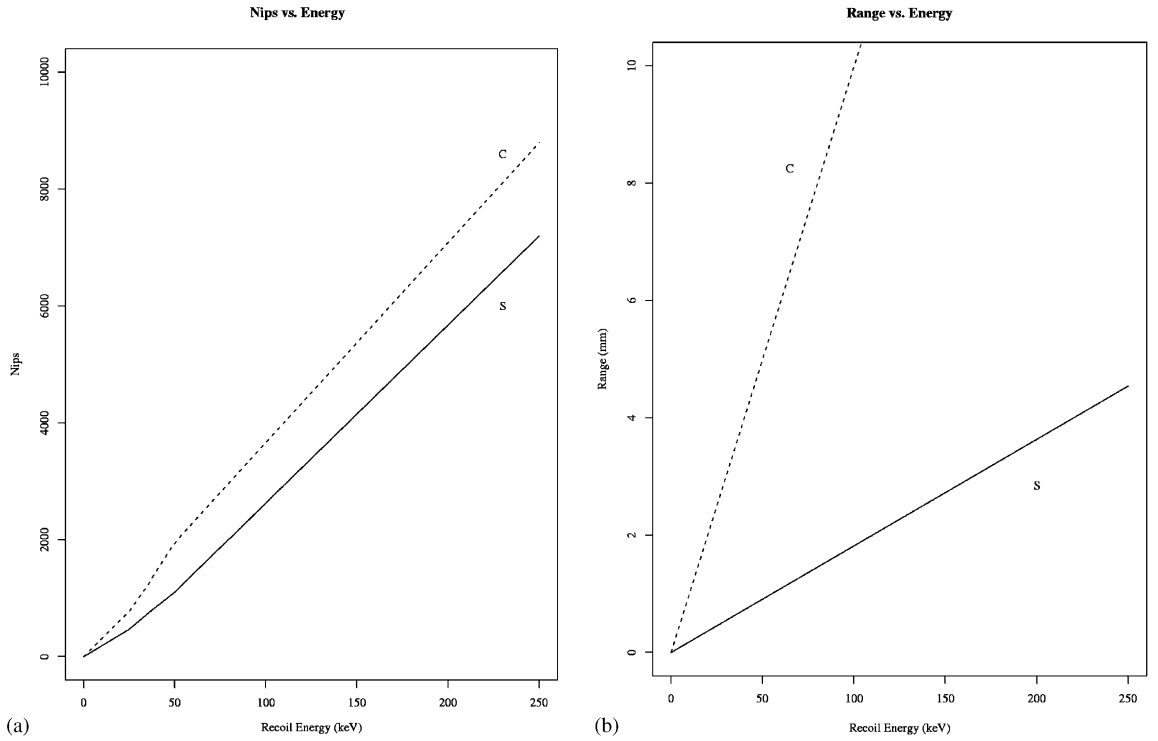

Fig. 9. $Nips(E_r)$ (a) and $R(E_r)$ (b) for S and C recoils.

windows was calculated for the data and the MC and compared. The reduced χ^2 for this comparison was 6.0. In order to improve the comparison the functions for $Nips(E_r)$, where E_r is the recoil energy, and $R(E_r)$ within the MC were allowed to be scaled for S and C recoils separately. A good fit was found when the $Nips(E_r)$ for S and C were multiplied by 1.25, the $R(E_r)$ for S multiplied by 0.5 and the $R(E_r)$ for C unchanged. This produced reduced χ^2s of 0.96 and 1.29 showing good agreement between data and MC. The resulting $Nips(E_r)$ and $R(E_r)$ functions are shown in Fig. 9 for S and C. The $Nips(E_r)$ is not strictly linear and it is felt that the non-linearity is an important component of the function. The $R(E_r)$ functions are linear with zero intercepts and slopes of 0.0182 mm/keV for S and 0.0998 mm/keV for C.

The *Nips* vs. R_2 plot for the MC based on these functions is shown in Fig. 10. This plot shows that the strong lower band in Fig. 6 is due to S recoils while the diffuse events above it are due to C recoils. The percentage of S(C) recoils in this simulation removed by the various cuts is shown as the middle(last) percentage in the list of cuts earlier. The large number of events cut by the *ZeroNipCut* is simply a reflection of the large software threshold and the prevalence of low energy recoils from a ^{252}Cf spectrum. It is not at odds with the statement made earlier about robustness of the neutron signal in the data to increases in the software threshold because that calculation was done only on events that produced more than 500 *Nips*. Ninety-seven percent of the S recoils that were cut by *ZeroNipCut* in the MC had less than 500 *Nips*. Overall 39% of the events survived the cuts. No attempt was made to model the effect of the 200 μS RC filter, shown in Fig. 3, on the data as any event neutron passing the 150 *DFNip* threshold would certainly pass the −75 mV hardware trigger threshold.

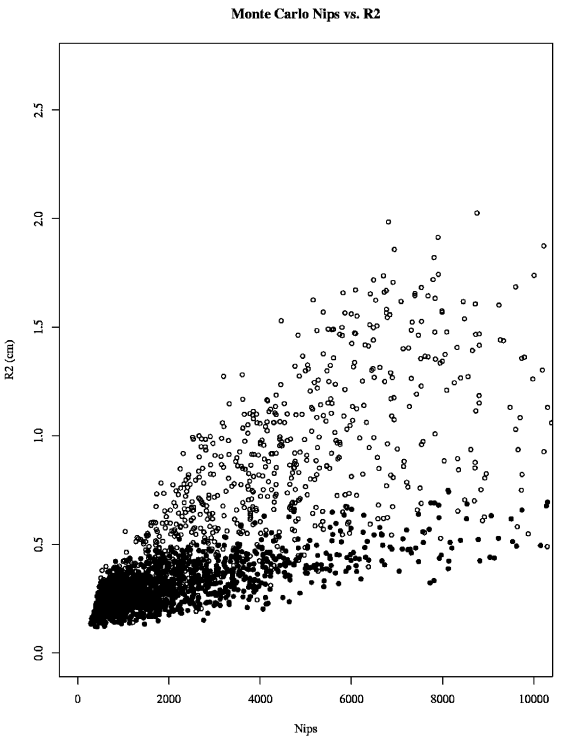

Fig. 10. *Nips* vs. R_2 from the MC. S recoils are shown with solid circles while C recoils are shown with open circles.

Acknowledgements

The authors gratefully acknowledge the help of Nate Villaume and Haick Issian in carrying out this research. This work was supported by the National Science Foundation, the Research Corporation, and Occidental College. Correspondence should be addressed to D.P. Snowden-Ifft.

References

[1] D.P. Snowden-Ifft, C.J. Martoff, J.M. Burwell, Phys. Rev. D 61 (2000) 1.
[2] C.J. Martoff, D. Snowden-Ifft, T. Ohnuki, N. Spooner, M. Lehner, Nucl. Instr. and Meth. A 440 (2000) 335.
[3] T. Ohnuki, C.J. Martoff, D.P. Snowden-Ifft, Nucl. Instr. and Meth. A 463 (2001) 142.
[4] H. Issian, Radiation Safety Officer Caltech, personal communication.
[5] Snowden-Ifft, unpublished.
[6] E.A. Lorch, Int. J. Appl. Radiat. Isot. 24 (1973) 585.
[7] R.J. Howarton, et al., UCRL 50 (1993) 400.
[8] G.L. Cano, Phys. Rev. 169 (1968) 277.
[9] J.F. Ziegler, J.P. Biersack, U. Littmark, The Stopping and Range of Ions in Solids, Pergamon Press, Oxford, England, 1985.
[10] G.E. Evans, P.M. Stier, C.F. Barnett, Phys. Rev. 90 (1953) 825.
[11] L. Rolandi, W. Blum, Particle Detection with Drift Chambers, Spring, Berlin, Germany, 1994, p. 146.